


SCIENTIFIC REPORTS



OPEN

New sedimentary evidence reveals a unique history of C₄ biomass in continental East Asia since the early Miocene

Bin Zhou¹, Michael Bird², Hongbo Zheng³, Enlou Zhang⁴, Christopher M. Wurster², Luhua Xie⁵ & David Taylor⁶

Pyrogenic carbon (PyC) and *n*-alkane data from sediments in the northern South China Sea reveal variations in material from C₄ plants in East Asia over the last ~19 Ma. These data indicate the likely presence of C₄ taxa during the earliest part of the record analysed, with C₄ species also prominent during the mid and late Miocene and especially the mid Quaternary. Notably the two records diverge after the mid Quaternary, when PyC data indicate a reduced contribution of C₄ taxa to biomass burning, whereas plant-derived *n*-alkanes indicate a greater abundance of C₄ plants. This divergence likely reflects differences in the predominant source areas of organic materials accumulating at the coring site, with PyC representing a larger source area that includes material transported in the atmosphere from more temperate (relatively cooler and drier) parts of East Asia. Variations in the relative abundances of C₃ and C₄ taxa appear to be linked to a combination of environmental factors that have varied temporally and geographically and that are unique to East Asia. A major expansion of C₄ biomass in warmer subtropical parts of eastern Asia from ~1 Ma and particularly from ~0.4 Ma is later than other parts of the world.

The Calvin-Benson cycle, the process through which plants convert inorganic carbon (C) and water to three C (C₃) sugar molecules, originated when atmospheric composition was very different from present^{1,2}. One modification to the cycle, leading to reduced photorespiration effects and improved photosynthetic efficiency under certain conditions (e.g. moisture stress and relatively low *p*CO₂), involves production of four C (C₄) oxaloacetate as the first-formed product of photosynthesis. Uncertainty surrounds the exact date of origin of this modification. That said, there is no widely accepted evidence of C₄ taxa pre-dating the Oligocene³, with molecular studies indicating that the C₄ photosynthetic pathway first appeared between 35 and 30 Ma⁴, a period that includes a major decline in *p*CO₂⁵. Only ~3% of angiosperm species currently support the C₄ pathway. However, despite being utilized by a relatively small proportion of the global flora, C₄ taxa – predominantly in the form of grasses – account for a substantial proportion of vegetation cover of Earth⁶, and include important food staples.

An expansion of plants utilising the C₄ photosynthetic pathway (e.g., tropical grasses) relative to those using the C₃ pathway (e.g., trees, shrubs and temperate grasses) in the late Miocene constitutes one of the most important biogeographical transformations of the Cenozoic^{7–10}. The timing of this expansion appears to have varied geographically, occurring later in East Asia than other parts of the world^{11–15}. As evidence has accumulated, however, the expansion of C₄ plants in East Asia appears to have been phased, rather than a single event, and may have occurred much earlier in some parts of the region^{16,17}, than in others¹⁸. Determining when and where the C₄ photosynthetic pathway first appeared on the Asian continent is difficult because direct evidence, in the form of plant remains such as pollen and phytoliths, is rare. Furthermore, when records are available, they are often

¹Key Laboratory of Surficial Geochemistry (Ministry of Education), School of Earth Sciences and Engineering, Nanjing University, Nanjing, China. ²College of Science and engineering and Centre for Tropical environmental and Sustainability Science, James Cook University, Cairns, Australia. ³School of Resource, Environment and Earth Science, Yunnan University, Chenggong District, Kunming, China. ⁴State Key Laboratory of Lake Science and Environment, Nanjing Institute of Geography and limnology, Chinese Academy of Sciences, Nanjing, China. ⁵CAS Key Laboratory of Marginal Sea Geology, Guangzhou Institute of Geochemistry, Chinese Academy of Sciences, Guangzhou, China. ⁶Department of Geography, National University of Singapore, Singapore, Singapore. Correspondence and requests for materials should be addressed to B.Z. (email: zhoubinok@nju.edu.cn)

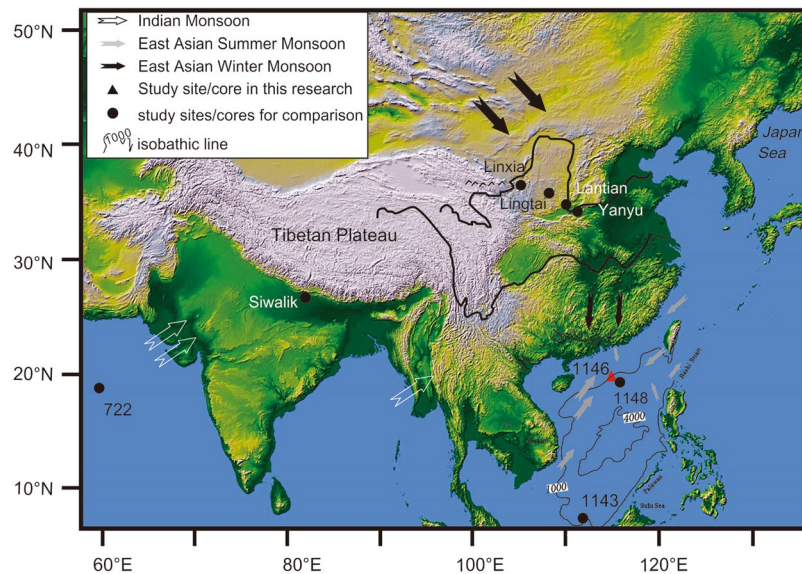


Figure 1. Map showing location of ODP Site 1146 and other important sites mentioned in the paper. The upper left panel contains the legend for the map. Ocean core locations ODP Site 1081 (South Atlantic, 19°37.2'S, 11°19.2'E, 793.8 m water depth), ODP site 717 (Bengal Fan, 0°56'S, 81°23'E, 4734.7 m water depth) and DSDP Leg 10 Site 94 (Gulf of Mexico, 24°20'N, 88°28.2'W, 1793 m water depth) mentioned in the text of the paper are not shown. The map was generated specifically for this paper using the ETOPO5 gridded elevation dataset (Version ETOPO5, <http://www.ngdc.noaa.gov/mgg/global/etopo5.HTML>) and Coreldraw (Version Coreldraw X7, <http://www.corel.com/cn>); no copyright problems are envisaged.

incomplete; C_4 taxa often occupy environments that are not conducive to the preservation of organic material *in situ*, and achieving a high level of certainty in distinguishing between many C_4 and C_3 taxa in pollen and phytolith records can be problematic.

Stable C isotope ($\delta^{13}C$) values for C_3 plants globally range between -37‰ and -20‰ (average -28.5‰)¹⁹, while the $\delta^{13}C$ values for C_4 plants range from -15‰ to -9‰ (average -13‰)^{20–22}. Pyrogenic carbon (PyC), also known as elemental carbon (EC) or black carbon (BC), is produced through the incomplete combustion of biomass and can preserve the original C isotope value of the parent plants²³. PyC is generally resistant to decomposition, and upon extraction from sediments can be used not only to document the frequency and intensity of past fire activity, but also changes in the relative contributions of C_4 and C_3 plants in combusted biomass^{15, 16, 23–25}. Similarly, long chain *n*-alkanes ($\geq n-C_{27}$), which are important building blocks of lipids forming the protective waxy cuticle covering leaf and stem tissue, are resistant to diagenetic alteration²⁶. Where herbaceous vegetation predominates, *n*-alkanes of C_{31} and C_{33} are abundant components of sediments, while larger proportions of *n*-alkanes of C_{27} and C_{29} are generally indicative of wooded and forested landscapes (i.e. C_3 taxa)^{27–29}. Thus ratios of measured levels of *n*-alkanes, such as C_{31}/C_{27} , can be used to reconstruct the relative contributions of herbaceous and woody plants to organic C preserved in sediments²⁷. Furthermore, although long chain *n*-alkanes typically have lower $\delta^{13}C$ values than bulk tissue³⁰, fractionation effects can be removed, so that the PyC and long chain *n*-alkanes composition of organic material in sediments can be used as a basis for inferring past variations in the relative abundances of C_3 and C_4 plants in, respectively, combusted biomass and vegetation^{23, 30, 31}.

The South China Sea (SCS), a marginal sea between Asia and the Pacific Ocean, is dominated climatically by the East Asian monsoon^{16, 32, 33}. Sediments accumulating on the bed of the northern SCS, largely supplied by major rivers but also including aeolian material transported by the East Asian Winter Monsoon (EAWM)³⁴, provide a potential source of information on environmental variations affecting continental East Asia during the late Cenozoic. To date, there is only one sediment-based record of variations in PyC from the northern SCS¹⁶. A second core, collected from a deep water site in the southern part of the SCS, has yielded a record of variations in *n*-alkane content of sediment, presumably largely of low latitude origin, for the last 5 Ma²⁹. Here we present new data in the form of variations in PyC and *n*-alkanes from the same sediment core from the northern SCS relating to the last ~19 Ma. These new data are compared with published information in order to describe and explain the unique history of C_3 and C_4 taxa in East Asia since the early Miocene.

Study area, materials and methods. The Ocean Drilling Program (ODP) Leg 184, Site 1146 (19°27.4'N, 116°16.4'E, 2092 m water depth) retrieved sediment from a small rift basin on the mid-continental slope of the northern SCS, located less than 50 km to the northeast of ODP Site 1147/1148 (Fig. 1). The sediment sequence obtained at ODP Site 1146 extended to a sub-seafloor depth of 643 m composite depth (mcd). For this study, a total of 149 2-cm-thick sample slices were collected at 4 m intervals between 641 mcd and the surface. Chronological control was established on the basis of palaeomagnetism and biostratigraphy³⁵ (S1, Supplementary material), with the ages of sample depths between control points established through linear interpolation (Fig. S1). According to the age-depth model for ODP Site 1146³⁵, the sequence of sediments between 641 mcd and the surface covers the

last ~19 Ma, with the sampling interval of 4 m adopted in the current research equating to a temporal resolution of ~100 ka.

PyC was extracted using the method of Gustafsson *et al.*³⁶. Sediment samples were pretreated with 1 M NaOH, HCl and HNO₃ to remove inorganic C and some of the organic forms that might lead to BC formation during the pre-combustion step. PyC was then measured following combustion at 375 °C in air for 24 h, with the $\delta^{13}\text{C}$ values for PyC ($\delta^{13}\text{C}_{\text{PyC}}$) values determined using a MAT-253 mass spectrometer. Isotopic compositions are expressed as deviations relative to the V-PDB standard with a precision of $\pm 0.2\%$ or better. This procedure differs from the oxidation method used to measure PyC (therein termed BC) in sediments from ODP Sites 1147/1148 and the Lingtai Section of the Chinese Loess Plateau (CLP)^{16,37}.

For analysis of high molecular weight *n*-alkanes, samples were freeze-dried before being ground manually. After adding an internal standard ($n\text{C}_{24}\text{D}_{50}$), a ~3 g sample was ultrasonically extracted in dichloromethane-methanol (3:1, v/v). Extracts were dried and saponified with 6% KOH-methanol. Hexane was then used to extract hydrocarbons, which were separated by column chromatography into the polar (i.e. alkanol) and non-polar (i.e. alkane) fractions. The $\delta^{13}\text{C}$ values for individual alkanes ($\delta^{13}\text{C}_{\text{Alk}}$) were determined using a GV Isochrom II system interfaced to a Hewlett-Packard 5890 gas chromatograph. The gas chromatograph was fitted with a fused Si column HP-5 MS (30 m-0.32 mm-0.25 mm) connected to the combustion interface. Helium was used as the carrier gas with a flow rate of 1.2 mL min⁻¹. The temperature was programmed to remain at 80 °C for 2 min, before rising to 220 °C at a rate of 10 °C min⁻¹, and then to 290 °C at a rate of 3 °C min⁻¹. The temperature was then maintained at 290 °C for 15 min. CO₂ was used as a reference gas, which was automatically introduced into the isotope ratio mass spectrometer before and after each analysis. The $\delta^{13}\text{C}$ values were calibrated against a standard mixture of *n*-alkanes ($n\text{C}_{12}$ - $n\text{C}_{32}$) of known isotopic composition (Indiana University, USA) and reported as ‰ relative to Vienna Pee Dee Belemnite (V-PDB). Replicate analyses showed that the standard deviation for each compound was less than 0.3‰. In order to maintain the reproducibility and accuracy of results, standards were run between samples, and each sediment sample was analyzed at least twice.

The $\delta^{13}\text{C}$ value of atmospheric CO₂ has not remained constant over time^{9,23,38,39}. Moreover, fractionation effects can occur during the production, transport and sedimentation of organic matter^{23,40,41}, and between atmospheric CO₂ and plant organic C, as well as varying between different taxa^{42,43}. These sources of variation introduce additional uncertainty into calculations of the relative contribution to combusted biomass and relative abundance in vegetation of C₄ taxa based on, respectively, $\delta^{13}\text{C}_{\text{PyC}}$ and $\delta^{13}\text{C}_{\text{Alk}}$, and hence need to be accounted for when interpreting records of ancient $\delta^{13}\text{C}$. Carbon isotopic enrichment factors for PyC and *n*-alkanes relative to atmospheric CO₂ ($\epsilon_{\text{PyC-CO}_2}$ and $\epsilon_{\text{Alk-CO}_2}$, respectively) were thus applied to calculate C₄ abundance in the current study (S2 and Fig. S2, Supplementary material).

Results

The PyC content of sediments from ODP Site 1146 (Fig. 2a, Table S1) shows an overall slight increase from the early Miocene through to the Quaternary, ranging from 0.014% to 0.16% (average 0.06%). This trend is superimposed upon strong variability in the data, with the amplitude of variation particularly large from the mid Quaternary. The latter period includes two intervals of high PyC content, centred upon ~1 Ma and 0.2 Ma. $\delta^{13}\text{C}_{\text{PyC}}$ values range from -25‰ to -17.2‰ (average -21.2‰), and also show an overall increase since the early Miocene, before declining after ~2 Ma (Fig. 2b, Table S1). Relatively high (less negative) $\delta^{13}\text{C}_{\text{PyC}}$ values date to the early Miocene (~18–19 Ma), mid Miocene (~14 Ma), late Miocene/early Pliocene (~7–4.5 Ma), and to the early to mid Quaternary (~2–1 Ma).

Trends in C₃₁/C₂₇ ratios (Fig. 2c, Table S1) are broadly similar to those exhibited by PyC; C₃₁/C₂₇ ratios vary over the last ~19 Ma, showing an overall slight increase to ~1 Ma, with an increased frequency of above average values after ~7.5 Ma, exhibiting greatest variability and highest values from ~1 Ma. In addition, C₃₁/C₂₇ ratios fluctuate through the early and mid Miocene, with four peaks around ~18 Ma, ~15.5 Ma, ~14 Ma and ~11 Ma.

The weighted mean $\delta^{13}\text{C}$ values of long chain alkanes, determined from $(nC_{27} * \delta^{13}\text{C}_{nC_{27}} + nC_{29} * \delta^{13}\text{C}_{nC_{29}} + nC_{31} * \delta^{13}\text{C}_{nC_{31}}) / (nC_{27} + nC_{29} + nC_{31})$, is abbreviated to $\delta^{13}\text{C}_{\text{Alk}}$. Values of $\delta^{13}\text{C}_{\text{Alk}}$ varied from -33.2‰ to -25.6‰ (average -29.9‰) (Fig. 2d, Table S1). Although fluctuating, an overall trend of declining (increasingly negative) values is evident, from the earliest parts of the record (~19 Ma) to the mid Quaternary, with three zones of relatively high (less negative) $\delta^{13}\text{C}_{\text{Alk}}$ values dating to around the early Miocene (18–19 Ma), late mid Miocene (11.5–12.5 Ma), and middle and later part of the late Miocene (~7.5–5.2 Ma). $\delta^{13}\text{C}_{\text{Alk}}$ values peak (least negative) after ~1 Ma, especially from 0.4 Ma. Over the entire sequence of sediments described here, trends in $\delta^{13}\text{C}_{\text{Alk}}$ values are generally opposite to those of $\delta^{13}\text{C}_{\text{PyC}}$, particularly from the early Quaternary and especially from ~1 Ma.

Variations in $\delta^{13}\text{C}$ value of atmospheric CO₂³⁹ (Fig. 2e), interpolated to correspond directly with dated $\delta^{13}\text{C}_{\text{PyC}}$ and $\delta^{13}\text{C}_{\text{Alk}}$ records, were used to derive estimates of $\epsilon_{\text{PyC-CO}_2}$ and $\epsilon_{\text{Alk-CO}_2}$, respectively. Conservative estimates of the relative contribution of C₄ taxa to combusted biomass and vegetation ranged from, respectively, 0–34.7% (average 12.9%) and 0–41.6% (average 9.9%) (Fig. 2f and g). Values of both $\epsilon_{\text{PyC-CO}_2}$ and $\epsilon_{\text{Alk-CO}_2}$ indicate the likely presence of C₄ taxa in East Asia during the early Miocene, later part of mid Miocene and the late Miocene through to the Late Quaternary. Some differences are evident in the two sources of information, however. The $\epsilon_{\text{PyC-CO}_2}$ data tend to indicate a relatively significant and continuous, though strongly varying, C₄ contribution to combusted biomass, especially when compared with the corresponding estimated abundance of C₄ taxa in terrestrial vegetation based on $\epsilon_{\text{Alk-CO}_2}$ data. The largest differences between the two datasets date to the Pliocene and Quaternary; $\epsilon_{\text{PyC-CO}_2}$ data indicate an overall substantial contribution of C₄ grasses to combusted biomass from the late Miocene through to the Quaternary, though with an overall decline evident after ~2 Ma. Lower $\epsilon_{\text{Alk-CO}_2}$ values indicate a predominance of C₃ grasses from around the beginning of the Pliocene through to ~1 Ma. This is supported to an extent by the enriched C₃₁/C₂₇ ratios, which suggest a greater herbaceous contribution to organic C from the late Miocene. An expansion of herbaceous vegetation generally (including a greater proportion of C₄

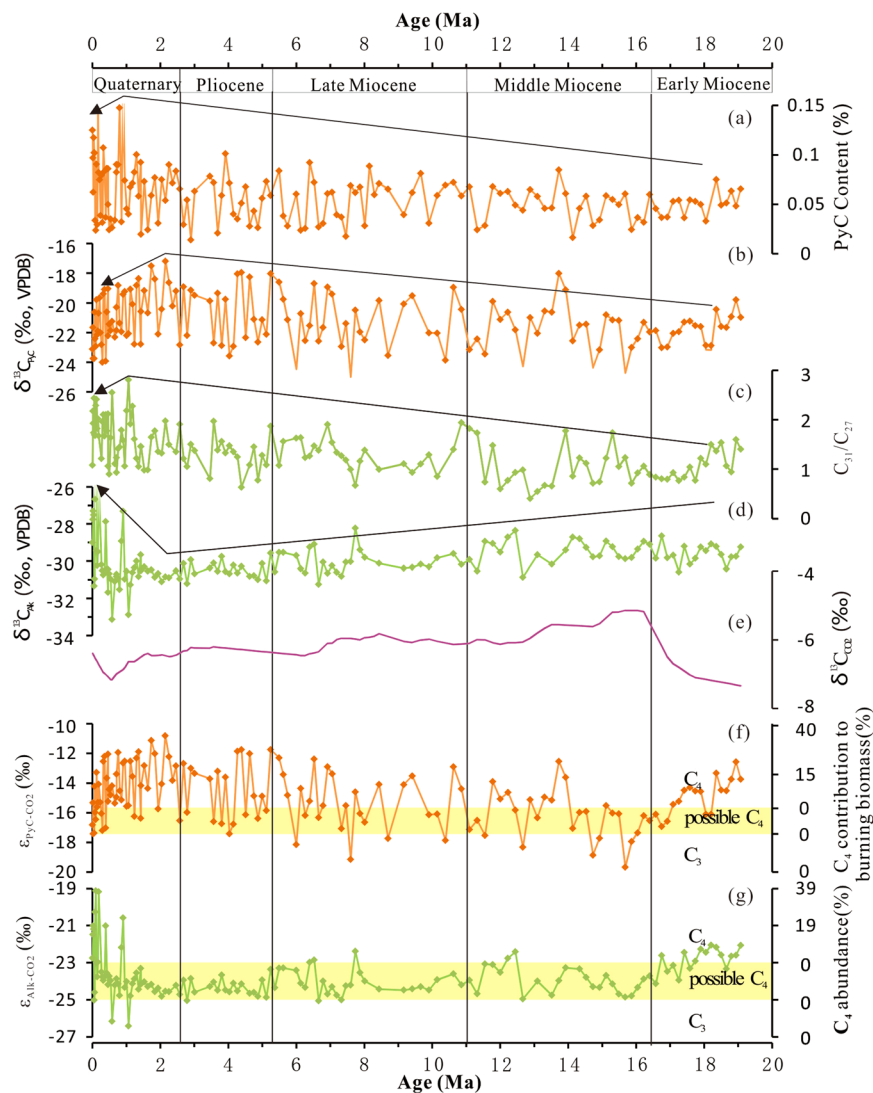


Figure 2. Abundance and carbon isotope composition data from *n*-alkanes and pyrogenic C (PyC) from ODP core 1146: (a) PyC content; (b) $\delta^{13}\text{C}$ values of PyC ($\delta^{13}\text{C}_{\text{PyC}}$); (c) $\text{C}_{31}/\text{C}_{27}$ *n*-alkane ratio; (d) Average $\delta^{13}\text{C}$ values of long-chain *n*-alkanes ($\delta^{13}\text{C}_{\text{Alk}}$); (e) Record of $\delta^{13}\text{C}$ of atmospheric CO_2 ³⁹; (f) The contribution of C_4 taxa to combusted biomass based on carbon isotopic enrichment factor for PyC ($\epsilon_{\text{PyC-CO}_2}$); (g) C_4 abundance based on carbon isotopic enrichment factor for *n*-alkanes ($\epsilon_{\text{Alk-CO}_2}$). Arrows indicate the overall trend in proxies. Two yellow bars show the area of uncertainty in reconstructing the relative prominence of C_3 and C_4 taxa based on $\epsilon_{\text{PyC-CO}_2}$ and $\epsilon_{\text{Alk-CO}_2}$, and thus the basis for the very conservative estimates of prominence of C_4 taxa mentioned in the text of this paper.

grasses at times) from ~1 Ma, particularly from ~0.4 Ma, is suggested by enriched high $\delta^{13}\text{C}_{\text{Alk}}$ data values and generally higher average $\text{C}_{31}/\text{C}_{27}$ ratios.

Discussion

Deviation of PyC and *n*-alkane records in ODP 1146 from northern SCS. Differences in *n*-alkane and PyC data from the same core likely reflect differences in both provenance of the C on which the measurements are based, and in the mode of transport of the C from the terrestrial source to the site of deposition. PyC is formed at high temperatures during the combustion of biomass and emitted to the atmosphere before a proportion is deposited in sedimentary environments⁴⁴, with the amount deposited dependent on atmospheric transport (influenced by wind velocity and direction and topography), precipitation and depositional processes. Several studies have indicated that PyC preserved in deep-sea sediments in the SCS originates via long-range transport from burning in central and southeastern Asia^{45–51} (S3, Supplementary material). Atmospheric transport from these sources is particularly active during EAWM, when dry continental conditions can also enhance the likelihood of vegetation fires^{52,53}. In general, highly seasonal and semi-arid climate conditions will result in biomass that is prone to burning, at least towards the end of the dry season, and, on occasion, in intense fires²⁴. Thus levels of PyC accumulating in sediments in the SCS are affected not only by the extent and composition of vegetation

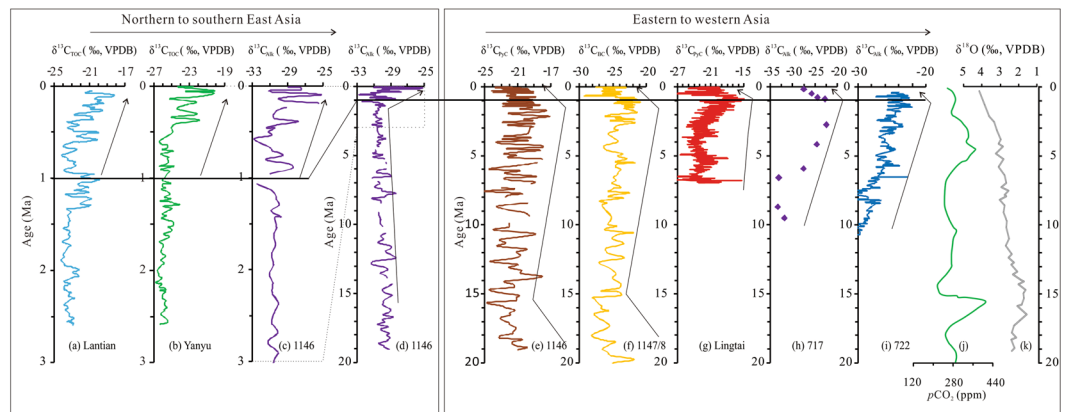


Figure 3. Summary of data for ODP core 1146 compared with similar data from sites proximate to, and on, the continent of Asia. Charts in the left panel summarise data north to south across East Asia. (a) and (b) $\delta^{13}\text{C}_{\text{TOC}}$ from transect sections on Chinese Loess Plateau (from northwest to southeast: Lantian, Yanyu)^{12, 18}; (c) and (d) $\delta^{13}\text{C}_{\text{alk}}$ values from core 1146 since the last 3 Ma and since about 19 Ma (this study). The right panel summarises data from a far larger area. (e) $\delta^{13}\text{C}$ values of PyC from core 1146 in this study; (f) and (g) $\delta^{13}\text{C}$ values of black carbon from 1147/8 and $\delta^{13}\text{C}$ values of PyC from Lingtai loess section^{16, 37}; (h) and (i) marine sediments in Indian Ocean (ODP 717)⁶² and Bengal Fan (ODP 722)⁶³; (j) Published $p\text{CO}_2$ records since the mid-Miocene based on a compilation of CO_2 curves (green line)⁵⁹; (k) Simplified composite $\delta^{18}\text{O}$ record of deep-sea benthic foraminifera as a proxy for global temperature variations⁶⁵. Dashed line shows in enlarged form the record for $\delta^{13}\text{C}_{\text{alk}}$ in core 1146 since the last ~3 Ma. Solid line highlights the divergence of $\delta^{13}\text{C}$ values occurring since the mid Quaternary. Arrows show direction of overall change in the data.

available for combustion, but also by burning regime and by variations in the EAWM in particular²⁴. Variations in PyC therefore likely represent an integration of conditions over a broad geographic area, with the source area of PyC accumulating in the northern SCS potentially including cold-adapted vegetation in more temperate, higher altitude and latitude parts of continental East Asia¹⁶. This is evident in similarities between variations in $\delta^{13}\text{C}_{\text{PyC}}$ measured at ODP Site 1146 discussed here and $\delta^{13}\text{C}_{\text{BC}}$ from Site 1148¹⁶, and from the CLP over the last ~7 Ma¹⁵ (Fig. 3).

By comparison, *n*-alkanes are mainly derived from plant leaves³⁰. Surface sediment *n*- C_{29} concentrations are in good agreement with data on pollen from approximately the same suite of modern sediments in the northern SCS^{54, 55}. The main delivery mechanism for *n*-alkanes is likely to be dominated by fluvial inputs and then marine currents via the Bashi and Taiwan straits⁵⁵. Some *n*-alkanes may also have been deposited from the atmosphere, along with aeolian dust and aerosols associated with biomass burning⁵⁶. However, the fact that levels of *n*-alkanes and PyC measured in the same sediment samples are not well-correlated suggests the two proxies have different provenances (Fig. S3). Possibly therefore, *n*-alkanes accumulating in the past in sediments in the northern SCS originated from relatively well-vegetated parts of subtropical East Asia, rather than as a result of long distance aeolian input from more temperate land to the north, where the vegetation cover is comparatively sparse²⁴. Catchments draining into the northern SCS are likely to be the dominant means by which organic material containing plant lipids is transported mainly from sub-tropical latitudes⁵⁵, with variations in $\delta^{13}\text{C}_{\text{Alk}}$ therefore affected by a different set of drivers to PyC abundance, including changes in monsoonal precipitation and fluvial discharge, catchment conditions and the extent and proximity of land relative to ocean⁵⁷.

Variations in C_4 contribution to vegetation and combusted biomass in East Asia recorded by PyC and *n*-alkane data. Variations in the prominence of C_4 taxa estimated from $\varepsilon_{\text{PyC-CO}_2}$ (relative contribution to combusted biomass) and $\varepsilon_{\text{Alk-CO}_2}$ (relative abundance in vegetation) are generally in phase with the $\delta^{13}\text{C}_{\text{PyC}}$ and $\delta^{13}\text{C}_{\text{Alk}}$ records, respectively. The $\delta^{13}\text{C}_{\text{PyC}}$ values are also in general agreement with variations in $\delta^{13}\text{C}_{\text{BC}}$ from ODP sites 1147/1148¹⁶ (Fig. 3), notwithstanding the aforementioned systematic offset in values due to differences in the analytical techniques employed²³. Variations in $\delta^{13}\text{C}_{\text{Alk}}$ are also within a similar range to that observed in a previously reported record from the northern SCS⁵⁷ covering a shorter period of time than that discussed here.

The presence of C_4 taxa during the early (~18.5 Ma) and mid Miocene (~14 Ma) and from the late Miocene (~7.5 Ma) is supported by existing data^{9, 15–17, 58}. Variations in abundances of C_4 taxa have been attributed to the changes in $p\text{CO}_2$ ^{10, 59} and to evolution of East Asian monsoon^{12, 16}, seasonality¹⁸, aridity and/or fires^{15, 58}. Intensification of the East Asian Summer Monsoon (EASM) is thought to date to about 24 Ma, with a peak in intensity during the mid Miocene, a weakening after ~8 Ma and strengthening again during the late Pliocene/early Quaternary^{29, 30}, while strengthening of the EAWM is thought to have occurred 16–14 Ma, ~8 Ma, and ~3 Ma and to have further intensified from the mid Quaternary⁶⁰. Increasing PyC content indicates rising levels of biomass burning, with periods of relatively high contributions to combusted biomass from C_4 taxa evident ~14 Ma, ~7–4.5 Ma and ~2.2–1.5 Ma. Increased contributions of C_4 taxa to biomass burning may represent a climatically promoted competitive advantage for C_4 photosynthesis, due not only to a strengthened EAWM and greater aridity^{57, 61}, but also to increased seasonality as a result of renewed intensification of the EASM, especially

from ~3 Ma. From the mid Quaternary, both above average PyC levels and C_{31}/C_{27} ratios could be a response to increased aridity, possibly due to a strengthening of the EAWM following further expansion of the northern hemisphere ice sheets^{12,29,32}. The contribution of C_4 taxa to combusted biomass declines from ~2 Ma, presumably because of a greater presence of C_3 plants in the source region for PyC. Evidence from the CLP for increased prominence of C_3 taxa during much of the Quaternary may represent a combination of a more intense EAWM and reduced temperatures during the main growing season in more temperate parts of the region, with both factors favouring C_3 photosynthesis^{15,62}.

At lower latitudes, C_3 taxa were prominent from the mid Miocene to the Pliocene/Quaternary boundary, under warm and humid climate conditions presumably owing to the influence of the EASM³³. Reduced moisture and increased seasonality from the late Pliocene through to ~1 Ma, with the majority of precipitation occurring during the growing season²⁹, could have facilitated sustained increases in the relative abundance of C_3 grasses, as evidenced by relatively lower $\epsilon_{\text{Alk-CO}_2}$ values and higher C_{31}/C_{27} ratios. As seasonal conditions developed and vegetation canopies became more open, expansion of C_4 biomass could have become tightly coupled in a feedback relationship to changes in burning regime and aridity that effectively selected against shrubs and trees (i.e. C_3 species) and promoted further expansion of grasslands in which C_4 taxa were prominent. An expansion of C_4 taxa in subtropical East Asia from ~1 Ma, and especially ~0.4 Ma, may have been triggered by increased seasonality, aridity and changes to the fire regime.

A synthesis of evidence for C_4 variations across Asia. $\delta^{13}\text{C}$ values from fossil enamel and soils from the northwestern CLP (the northeastern margin of the Qinghai–Tibet Plateau) suggest increased abundance of C_4 taxa from ~3 Ma, with C_4 taxa becoming a significant component of the local vegetation around ~1.0 Ma¹³. An expansion of C_4 biomass ~1.0 Ma and, at lower altitude, ~0.4 Ma, on the southeastern parts of the CLP is evident in $\delta^{13}\text{C}$ data from Yanyu (620 m amsl) and Lantian (769 m amsl)^{12,18} (Fig. 3). The evidence from Lantian and Yanyu is thus consistent with our $\delta^{13}\text{C}_{\text{Alk}}$ data from the northern SCS.

The $\delta^{13}\text{C}$ values of n -alkanes obtained from palaeosols associated with the Siwalik Group and marine sediments from the Indus (ODP Site 722) and Bengal (ODP Site 717C) fans^{63,64}, dating to 12–11 Ma, indicate a predominantly C_3 flora during the mid Miocene (Fig. 3). A subsequent expansion of C_4 taxa during the late Miocene in western and southern Asia has been linked to aridification⁶⁴, although other factors, such as increased burning^{15,25} and lower $p\text{CO}_2$ may have played a role. Evidence of an expansion of C_4 biomass from ~8–6 Ma that peaked in the early to mid Quaternary in Asia, the South Atlantic (ODP Site 1081)⁶⁵, and Gulf of Mexico (DSDP Site 94)⁹ implies the possible effect of global decreases in moisture availability along with ice sheet formation and expansion that commenced during the late Miocene, as recorded in $\delta^{18}\text{O}$ variations preserved in the tests of foraminifera⁶⁶.

The detailed reconstruction of variations in the prominence of C_4 taxa estimated from $\epsilon_{\text{PyC-CO}_2}$ and $\epsilon_{\text{Alk-CO}_2}$ is limited by a number of uncertainties, including the effects of changes in atmospheric $p\text{CO}_2$ and fractionation due to moisture stress⁴², and potentially also O_2/CO_2 ratios⁶⁷. Notwithstanding these uncertainties, the available evidence is broadly consistent with the conclusion that the rise to prominence of C_4 taxa over a substantial proportion of subtropical East Asia differed in timing, likely reflecting local differences in the relative strengths of the suite of potential causal factors. Beginning in the late Pliocene, increased seasonality – with the majority of precipitation occurring during the growing season – and aridity overall could have facilitated sustained increases in the relative abundance of open vegetation in which C_4 taxa were important components. As seasonal climate conditions developed and vegetation canopies became more open, expansion of C_4 biomass may have become tightly coupled in a feedback relationship with changes in burning regime that effectively selected against shrubs and trees (i.e., C_3 species) and promoted further expansions of C_4 grasslands^{15,64,68}. Lower temperatures associated with continued uplift of central Asia coupled with a strengthened EAWM and the effects of fluctuating Quaternary ice sheets after ~2 Ma could have shifted habitats previously characterized by a relatively high proportion of C_4 taxa back within an envelope of environmental conditions that were more suited to C_3 species. From around the same time, but at lower altitudinal and subtropical parts of the region, aridity, enhanced by an expanded coverage of ice in the NH and large-scale hydrological dynamics, may have forced an abrupt expansion of C_4 biomass²⁹, thereby contributing to a history of C_3/C_4 variations in East Asia that is unique for the continent and more widely.

Conclusions

The abundance and C isotope composition of n -alkanes and PyC in samples from a sediment core from the northern SCS are used to reconstruct a history of variations in the relative prominence of C_4 and C_3 taxa in East Asia over the last ~19 Ma. Although present throughout the record, C_4 taxa appear to have been prominent at times during the Miocene and especially from the late Pliocene to mid Quaternary. However, n -alkane (a proxy of relative contribution to vegetation) and PyC (a proxy of relative contribution to combusted biomass) isotope data diverge from the mid Quaternary, most likely reflecting differences in provenance, with PyC representing a larger source area that includes higher altitude and more temperate parts of the region, and atmospheric processes as the primary means of transporting organic material from the interior of the continent to the coring site. Temperatures in these already cooler parts of the continent appear to have fallen to levels too low to support C_4 taxa from the mid Quaternary. New evidence presented in this paper in the context of existing data indicates that variations in the level and seasonality of rainfall and associated changes in biomass burning appear to have been important drivers of changes in the relative contributions of C_3 and C_4 taxa to East Asian vegetation throughout much of the past ~19 Ma. An expansion of C_4 taxa at low altitude/latitude from ~1 Ma, and especially ~0.4 Ma, may have been triggered by increased aridity and changes to the fire regime. This expansion commenced more recently than in other parts of the tropics and sub-tropics, and is one characteristic of a novel history of variations in C_3 and C_4 taxa in continental East Asia.

References

- Ehleringer, J., Sage, R., Flanagan, L. & Pearcy, R. Climate change and the evolution of C₄ photosynthesis. *Trends in Ecology and Evolution* **6**, 95–99 (1991).
- Bekker, A. *et al.* Dating the rise of atmospheric oxygen. *Nature* **427**, 117–120 (2004).
- Sage, R. & Stata, M. Photosynthetic diversity meets biodiversity: the C₄ plant example. *Journal of Plant Physiology* **172**, 104–119 (2015).
- Christin, P., Osborne, C., Sage, R., Arakaki, M. & Edwards, E. C₄ eudicots are not younger than C₄ monocots. *Journal of Experimental Botany* **62**, 3171–3181 (2011).
- Pagani, M., Zachos, J., Freeman, K., Tiplle, H. & Bohaty, S. Marked decline in atmospheric carbon dioxide concentrations during the Palaeogene. *Science* **309**, 600–603 (2005).
- Grace, J., San, J., Meir, P., Miranda, H. & Montes, R. Productivity and carbon fluxes of tropical savannas. *Journal of Biogeography* **33**, 387–400 (2006).
- Quade, J., Cerling, T. & Bowman, J. Development of Asian monsoon revealed by marked ecological shift during the latest Miocene in northern Pakistan. *Nature* **342**, 163–166 (1989).
- Cerling, T. *et al.* Global vegetation change through the Miocene/Pliocene boundary. *Nature* **389**, 153–158 (1997).
- Tiplle, B. & Pagani, M. A 35 Myr North American leaf-wax compound-specific carbon and hydrogen isotope record: implications for C₄ grasslands and hydrologic cycle dynamics. *Earth and Planetary Science Letters* **299**, 250–262 (2010a).
- Edwards, E., Osborne, C., Strömberg, C., Smith, S. & C₄ Grasses Consortium. The origins of C₄ grasslands, Integrating evolutionary and ecosystem science. *Science* **328**, 587–591 (2010).
- Ding, Z. & Yang, S. C₃/C₄ vegetation evolution over the last 7.0 Myr in the Chinese Loess Plateau, evidence from pedogenic carbonate δ¹³C. *Palaeogeogr. Palaeoclim. Palaeoecol.* **160**, 291–299 (2000).
- An, Z. *et al.* Multiple expansions of C₄ plant biomass in East Asia since 7 Ma coupled with strengthened monsoon circulation. *Geology* **33**, 705–708 (2005).
- Wang, Y. & Deng, T. A 25 m.y. isotopic record of paleodiet and environmental change from fossil mammals and paleosols from the NE margin of the Tibetan Plateau. *Earth and Planetary Science Letters* **236**, 322–338 (2005).
- Passey, B. *et al.* Strengthened East Asian summer monsoons during a period of high-latitude warmth? Isotopic evidence from Mio-Pliocene fossil mammals and soil carbonates from northern China. *Earth and Planetary Science Letters* **277**, 443–452 (2009).
- Zhou, B. *et al.* Late Pliocene–Pleistocene expansion of C₄ vegetation in semi-arid East Asia linked to increased burning. *Geology* **42**, 1067–1070 (2014).
- Jia, G., Peng, P., Zhao, Q. & Jian, Z. Changes in terrestrial ecosystem since 30 Ma in East Asia: stable isotope evidence from black carbon in the South China Sea. *Geology* **31**, 1093–1096 (2003).
- Zhang, Y., Xiong, S., Ding, Z., Lu, H. & Jiang, W. Carbon-oxygen isotope records of pedogenic carbonate from the Early Miocene–Pleistocene loess-red clay in the vicinity of the Liupanshan region and its implications for the early origin of C₄ plants in the Chinese Loess Plateau. *Quaternary Sciences* **31**, 800–811 (2011).
- Sun, J., Lu, T., Zhang, Z., Wang, X. & Lu, W. Stepwise expansions of C₄ biomass and enhanced seasonal precipitation and regional aridity during the Quaternary on the southern Chinese Loess Plateau. *Quaternary Science Reviews* **34**, 57–65 (2012).
- Kohn, M. J. Carbon isotope composition of terrestrial C₃ plants as indicators of (paleo) ecology and (paleo) climate. *Proceedings of the National Academy of Sciences USA* **107**, 19691–19695 (2010).
- Deines, P. The isotopic composition of reduced organic carbon in Handbook of environmental isotope Geochemistry I, the terrestrial environment (ed. Fritz, P. & Fontes, J. C.) 329–406 (1980).
- Liu, W. *et al.* Carbon isotopic composition of modern soil and paleosol as a response to vegetation change on the Chinese Loess Plateau. *Sci China Ser D–Earth Sci* **48**, 93–99 (2002).
- Wang, G., Feng, X., Han, J., Zhou, L., Tan, W. & Su, F. Paleovegetation reconstruction using δ¹³C of Soil Organic Matter. *Biogeosciences* **5**, 1325–1337 (2008).
- Bird, M. & Gröcke, D. Determination of the abundance and carbon isotope composition of elemental carbon in sediments. *Geochimica et Cosmochimica Acta* **61**, 3413–3423 (1997).
- Zhou, B. *et al.* The history of wildfire in the Chinese Loess Plateau during the last 420 ka and its implications to environmental and climate changes. *Palaeogeography, Palaeoclimatology, Palaeoecology* **252**, 617–625 (2007).
- Kim, D., Lee, Y., Hyeong, K. & Yoo, C. M. Terrestrial biome distribution in the Late Neogene inferred from a black carbon record in the northeastern equatorial Pacific. *Scientific Reports* **6**, 32847 (2016).
- Bird, M. *et al.* Terrestrial vegetation change inferred from *n*-alkane ¹³C analysis in the marine environment. *Geochimica et Cosmochimica Acta* **59**, 2853–2858 (1995).
- Cranwell, P. Chain-length distribution of *n*-alkanes from lake sediments in relation to post-glacial environmental change. *Freshwater Biol.* **3**, 259–265 (1973).
- Meyers, P. Applications of organic geochemistry to paleolimnological reconstructions: A summary of Examples from the Laurentian Great Lakes. *Organic Geochemistry* **34**, 261–289 (2003).
- Li, L., Li, Q., Tian, J., Wang, H. & Wang, P. Low latitude hydro-climatic changes during the Plio-Pleistocene: evidence from high resolution alkane records in the southern South China Sea. *Quaternary Science Reviews* **78**, 209–224 (2013).
- Collister, J., Rieley, G., Stern, B., Eglinton, G. & Fry, B. Compound-specific δ¹³C analysis of leaf lipids from plants with differing carbon dioxide metabolism. *Organic Geochemistry* **21**, 619–627 (1994).
- Zech, M. & Glaser, B. Improved compound-specific δ¹³C analysis of *n*-alkanes for application in palaeoenvironmental studies. *Rapid Communications in Mass Spectrometry* **22**, 135–142 (2008).
- Wang, P. *et al.* Evolution and variability of the Asian monsoon system: state of the art and outstanding issues. *Quaternary Science Reviews* **24**, 595–629 (2005).
- Clift, P., Wan, S. & Bluxtajn, J. Reconstructing chemical weathering, physical erosion and monsoon intensity since 25 Ma in the northern South China Sea: A review of competing proxies. *Earth-Science Reviews* **130**, 86–102 (2014).
- Wan, S., Li, A., Clift, P. & Stuut, J. Development of the East Asian monsoon: Mineralogical and sedimentologic records in the northern South China Sea since 20 Ma. *Palaeogeography, Palaeoclimatology, Palaeoecology* **254**, 561–582 (2007).
- Shipboard Scientific Party. Site 1146. Proceedings of the Ocean Drilling Program, Part A: Initial Reports, 184 (2000).
- Gustafsson, O. *et al.* Evaluation of a protocol for the quantification of black carbon in sediments. Global. *Biogeochemical Cycles* **15**, 881–890 (2001).
- Zhou, B., Shen, C., Zheng, H. & Zhao, M. Vegetation evolution on the central Chinese Loess Plateau since late Quaternary evidenced by elemental carbon isotopic composition. *Chinese Science Bulletin* **54**, 2082–2089 (2009).
- Farquhar, G., Ehleringer, J. & Hubick, K. Carbon isotope discrimination and photosynthesis. *Annu. Rev. Plant Physiol. Mol. Biol.* **40**, 503–537 (1989).
- Tiplle, B., Meyers, S. & Pagani, M. Carbon isotope ratio of Cenozoic CO₂: A comparative evaluation of available geochemical proxies. *Paleoceanography* **25**, PA3202 (2010b).
- Bird, M. & Ascough, P. Isotopes in pyrogenic carbon: A review. *Organic Geochemistry* **42**, 1529–1539 (2012).
- Liu, L., Yang, S., Cui, L. & Hao, Z. Stable carbon isotopic composition of black carbon in surface soil as a proxy for reconstructing vegetation on the Chinese Loess Plateau. *Palaeogeography, Palaeoclimatology, Palaeoecology* **388**, 109–114 (2013).

42. Schubert, B. & Jahren, H. The effect of atmospheric CO₂ concentration on carbon isotope fractionation in C₃ land plants. *Geochimica et Cosmochimica Acta* **96**, 29–43 (2012).
43. Schubert, B. & Jahren, H. Global increase in plant carbon isotope fractionation following the Last Glacial Maximum caused by increase in atmospheric pCO₂. *Geology* **43**, 435–438 (2015).
44. Thevenon, F. *et al.* Combining charcoal and elemental black carbon analysis in sedimentary archives: Implications for past fire regimes, the pyrogenic carbon cycle, and the human–climate interactions. *Global & Planetary Change* **72**, 381–389 (2010).
45. Ma, P., Gattiker, J., Liu, X. & Rasch, P. A novel approach for determining source-receptor relationships in model simulations: a case study of black carbon transport in northern hemisphere winter. *Environmental Research Letters* **8**, 24042–24049 (2013).
46. Lee, Y. *et al.* An integrated approach to identify the biomass burning sources contributing to black carbon epidemics in Hong Kong. *Atmospheric Environment* **80**, 478–487 (2013).
47. Luo, X. *et al.* Polycyclic aromatic hydrocarbons in suspended particulate matter and sediments from the Pearl River Estuary and adjacent coastal areas, China. *Environmental Pollution* **139**, 9–20 (2006).
48. Chuang, M. *et al.* Aerosol chemical properties and related pollutants measured in Dongsha Island in the northern South China Sea during –SEAS/Dongsha Experiment. *Atmospheric Environment* **78**, 82–92 (2013).
49. Lin, N. *et al.* An overview of regional experiments on biomass burning aerosols and related pollutants. *Atmospheric Environment* **78**, 1–19 (2013).
50. Wang, S. *et al.* First detailed observations of long-range transported dust over the northern South China Sea. *Atmospheric Environment* **45**, 4804–4808 (2011).
51. Wang, S. *et al.* Origin, transport, and vertical distribution of atmospheric pollutants over the northern South China Sea during the 7-SEAS/Dongsha Experiment. *Atmospheric Environment* **78**, 124–133 (2013).
52. Wang, L. *et al.* East Asian monsoon climate during the Late Pleistocene: high-resolution sediment records from the South China Sea. *Marine Geology* **156**, 145–284 (1999).
53. Wu, D. *et al.* Black carbon over the South China Sea and in various continental locations in South China. *Atmos. Chem. Phys.* **13**, 12257–12270 (2013).
54. Sun, X. & Li, X. A pollen record of the last 37 ka in deep sea core 17940 from the northern slope of the South China Sea. *Marine Geology* **156**, 227–244 (1999).
55. Pelejero, C. Terrigenous n-alkane input in the South China Sea: High-resolution records and surface sediments. *Chemical Geology* **200**, 89–103 (2003).
56. Zhao, Y. *et al.* Non-polar organic compounds in marine aerosols over the northern South China Sea: Influence of continental outflow. *Chemosphere* **153**, 332–339 (2016).
57. Zhou, B. *et al.* Climate and vegetation variations since the LGM recorded by biomarkers from a sediment core in the northern South China Sea. *Journal of Quaternary Science* **27**, 948–955 (2012).
58. Keeley, J. & Rundel, P. Fire and the Miocene expansion of C₄ grasslands. *Ecology Letters* **8**, 683–690 (2005).
59. Beerling, D. & Royer, D. Convergent Cenozoic CO₂ history. *Nature Geoscience* **4**, 418–420 (2011).
60. An, Z., Kutzbach, J., Prell, W. & Porter, S. Evolution of Asian monsoons and phased uplift of the Himalayan Plateau since Late Miocene times. *Nature* **411**, 62–66 (2001).
61. Guo, Z. *et al.* Onset of Asian desertification by 22 Myr ago inferred from loess deposits in China. *Nature* **416**, 159–163 (2002).
62. Zhang, Z., Zhao, M., Lu, H. & Faiia, A. Lower temperature as the main cause of C₄ plant declines during the glacial periods on the Chinese Loess Plateau. *Earth and Planetary Science Letters* **214**, 467–481 (2003).
63. Freeman, K. & Colarusso, L. Molecular and isotope records of C₄ grassland expansion in the late Miocene. *Geochimica et Cosmochimica Acta* **65**, 1439–1454 (2001).
64. Huang, Y., Clemens, S., Liu, W., Wang, Y. & Prell, W. Large-scale hydrological change drove the late Miocene C₄ plant expansion in the Himalayan foreland and Arabian Peninsula. *Geology* **35**, 531–534 (2007).
65. Hoetzel, S., Dupont, L., Schefuß, E., Rommerskirchen, F. & Wefer, G. The role of fire in Miocene to Pliocene C₄ grassland and ecosystem evolution. *Nature Geoscience* **6**, 1027–1030 (2013).
66. Zachos, J., Pagani, M., Sloan, L., Thomas, E. & Billups, K. Trends, rhythms and aberrations in global climate. *Science* **292**, 686–693 (2001).
67. Beerling, D., Lake, J., Berner, R., Hickey, I., Taylor, D. & Royer, D. Carbon isotope evidence implying high O₂/CO₂ ratios in the Permo-Carboniferous atmosphere. *Geochimica et Cosmochimica Acta* **21**, 3757–3767 (2002).
68. Strömberg, C. Evolution of grasses and grassland ecosystems. *Annual Review of Earth and Planetary Sciences* **39**, 517–544 (2011).

Acknowledgements

This research used samples and data provided by the IODP. The authors are grateful to Gangjian Wei, Jia Guodong, Wang Guoan and Liu Weiguo for beneficial discussions and suggested revisions to an earlier version of the paper. We appreciate the assistance of Yuhong Liao, Huashan Chen, Hui Wang, Ling Li, Yingfeng Xu and Yinhua Pan in the laboratory. All $\delta^{13}\text{C}_{\text{Alk}}$ analyses were conducted in the State Key Laboratory of Organic Geochemistry (SKLOG), Guangzhou Institute of Geochemistry, Chinese Academy of Sciences, while $\delta^{13}\text{C}_{\text{TOC}}$ and $\delta^{13}\text{C}_{\text{PyC}}$ analyses were conducted in the State Key Laboratory of Lake Science and Environment, Nanjing Institute of Geography and Limnology, Chinese Academy of Sciences. The support of the National Key Basic Research Program of China (2015CB953800), the National Natural Science Foundation of China (41172149, 40802034), Science Fund for Creative Research Groups of NSFC (41321062), State Scholarship Fund of China Scholarship Council (No. 2011832365) and the National University of Singapore and James Cook University, Australia, is also gratefully acknowledged.

Author Contributions

Bin Zhou and Hongbo Zheng organized the collection and analysis of samples from core ODP 1146 and designed the research. Bin Zhou, David Taylor and Michael Bird decided upon the focus and scope of this paper. Bin Zhou, David Taylor, Michael Bird and Christopher Wurster drafted the written content of the paper in consultation with the other co-authors. Enlou Zhang measured and analyzed the PyC content of sediment samples, while Luhua Xie measured and analyzed n-alkanes content. All co-authors were involved in interpreting the data and are in agreement with the interpretations arrived at, and conclusions drawn from the research. All co-authors have approved content of the article, and confirm that there are no conflicts of interest relating to the research described.

Additional Information

Supplementary information accompanies this paper at doi:10.1038/s41598-017-00285-7

Competing Interests: The authors declare that they have no competing interests.

Publisher's note: Springer Nature remains neutral with regard to jurisdictional claims in published maps and institutional affiliations.



This work is licensed under a Creative Commons Attribution 4.0 International License. The images or other third party material in this article are included in the article's Creative Commons license, unless indicated otherwise in the credit line; if the material is not included under the Creative Commons license, users will need to obtain permission from the license holder to reproduce the material. To view a copy of this license, visit <http://creativecommons.org/licenses/by/4.0/>

© The Author(s) 2017